



## Computational Investigations on IR, UV-VIS and NMR Spectra of Copper(II) Phenanthroline Complexes with DFT Method

*Koray SAYIN*

*Department of Chemistry, Faculty of Science, Cumhuriyet University, 58140 Sivas, Turkey*

Received: 04.05.2017; Accepted: 16.08.2017

<http://dx.doi.org/10.17776/csj.349259>

**Abstract:** Computational investigations were done on two Cu(II) complexes. There is no any data or spectral results of them in literature. In this paper, B3LYP one of the hybrid DFT functions was selected for mentioned complexes. Optimized structures, IR, UV-VIS and NMR spectrum of studied complexes were calculated and were calculated and examined in detail. Additionally, molecular electrostatic potential (MEP) maps, MEP contours and single occupied molecular orbitals (SOMO) were analyzed. Interaction energies between ligands and the metal atom, formation enthalpies and formation Gibbs free energies were investigated. Geometric structure and structural parameters were determined by computational techniques and the structures were supported by spectral analyses. The most reactive regions of mentioned complexes were determined by MEP maps and MEP contours.

**Keywords:** Cu(II) complexes, DFT studies, Spectral Studies, MEP mapss.

## DFT Yöntemi ile Bakır(II) Fenantrolin Komplekslerinin IR, UV-VIS ve NMR Spektrumları Üzerine Hesaplamalı Araştırmalar

**Özet:** İki Cu(II) kompleksleri üzerine hesapsal araştırmalar yapıldı. Literatürde, bu kompleksler hakkında herhangi bir bilgi yada spektral sonuçlar yoktur. Bu çalışmada, hibrit DFT fonksiyonellerinden biri olan B3LYP söz konusu komplekslerin hesaplarında kullanıldı. Söz konusu komplekslerin optimize yapıları hesaplandı ve IR, UV-VIS ve NMR spektrumları hesaplandı ve detaylı bir şekilde incelendi. İlaveten, doğrusal olmayan optik özellikler, moleküler elektrostatik potansiyel (MEP) haritaları, MEP konturları ve tek dolu moleküler orbitalleri analiz edildi. Ligand ve metal atom arasındaki etkileşim enerjileri, oluşum entalpileri ve Gibbs serbest enerjisi araştırıldı. Geometrik yapı ve yapısal parametreler hesapsal tekniklerle belirlendi ve komplekslerin yapıları spektral analizler ile desteklendi. Söz konusu komplekslerin en aktif bölgeleri MEP haritaları ve MEP konturları ile belirlendi.

**Anahtar Kelimeler:** Cu(II) kompleksleri, DFT çalışması, Spektral çalışma, MEP haritası.

### 1. INTRODUCTION

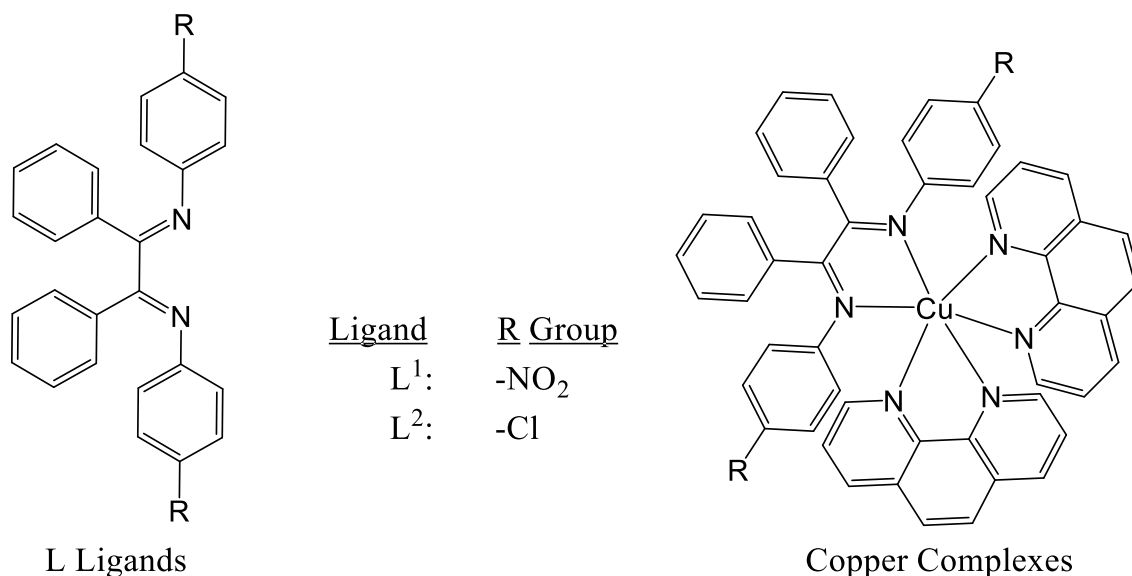
New Schiff bases and their complexes are currently attracting the attention of medical chemistry [1-6]. Metal complexes are known to accelerate the drug interaction with appropriate structure and the efficiency of a therapeutic agent can often be increased upon coordination with metal ions [7]. Pharmacological activity

has also been obtained to be highly dependent on environment and nature of the center atom and donor sequence of the ligands as different ligands exhibit different biological reactivity.

Biological reactivities of two ligands ( $L^1$  and  $L^2$ ) and their two complexes ( $[CuL^1(phen)_2]$  and  $[CuL^2(phen)_2]$ ) have been investigated towards some bacterias which are (*S. aureus*,

K. pneumonia, E. coli, P. aeruginosa, S. podity) and some fungus which are (A. niger, F. solani, C. lunata, R. bataicola, C. albicans) by Raman and Mahalakshmi in 2014 [8]. Schematic diagram of investigated complexes is represented in Scheme 1. Additionally,

[ZnL1(phen)2], [ZnL2(phen)2], [NiL1(phen)2] and [NiL2(phen)2] complexes have been studied as computationally by Sayin et. al in 2015 [9]. However, there is no any data about studied complexes in literature.



**Scheme 1.** Schematic diagram of studied Cu(II) complexes.

Quantum chemical investigations are attracted the interest of researchers and have been popular in recent years [10-14]. The goal of this paper, the structures of investigated complexes is firstly determined at the B3LYP method and geometric parameters are obtained from the optimized structure. Then, these structures are supported by IR and NMR spectrum. Additionally, UV-VIS spectrum of studied complexes are calculated. The single occupied molecular orbital (SOMO), molecular electrostatic potential (MEP) maps and MEP contours are investigated and examined in detail.

## 2. COMPUTATIONAL DETAILS

All computational processes of Cu(II) complexes were performed by using GaussView 5.0.8 [15], Gaussian 09 AML64-G09 Revision-C01 programs [16] and ChemBioDraw Ultra Version (13.0.0.3015)

[17]. Firstly, geometries of investigated complexes were fully optimized by using UFF force field which is one of the molecular mechanics methods [18]. UFF calculations were performed to gaining job time and prevent convergence problems at mentioned level. After that, the geometries of mentioned complexes reoptimized at density functional theory (DFT) method which is B3LYP [19,20] methods with LANL2DZ [21-23] for metal atoms and 6-31G(d,p) basis set for the rest atoms in complex structures. The vibrational frequency analyses indicate that optimized structures of relevant complexes were at stationary points corresponding to local minima without imaginary frequencies. Time dependent–density functional theory (TD-DFT) method was used for UV-VIS spectra calculations and GIAO method for NMR calculations of mentioned complexes.

Tetramethylsilane (TMS) was used as the reference substance for NMR calculations.

### 3. RESULTS and DISCUSSION

#### 3.1. Optimized Structures and Thermodynamic Parameters

The fully optimizations are done on  $[\text{CuL}^1(\text{phen})_2]$  (**1**) and  $[\text{CuL}^2(\text{phen})_2]$  (**2**) by using UFF and B3LYP methods with GEN keyword in vacuo. The optimized structures of complex (**1**) and complex (**2**) are presented in Fig. 1. In these figures, hydrogen atoms are omitted for clarity. Additionally, calculated structural parameters of investigated complexes are given in Table 1.

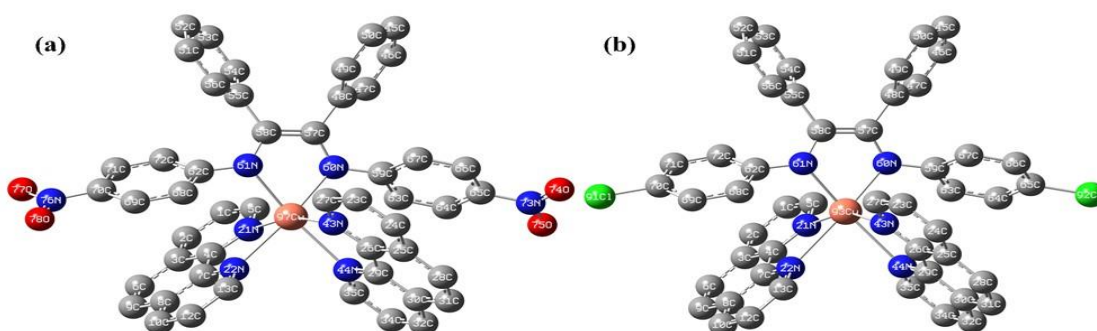


**Figure 1.** Optimized structures of (a)  $[\text{CuL}^1(\text{phen})_2]$  and (b)  $[\text{CuL}^2(\text{phen})_2]$  complexes at B3LYP method in vacuum with atomic labelling.

**Table 1.** The calculated structural parameters of mentioned complexes at B3LYP method with mix basis set in vacuum.

	Complex (1)	Complex (2)
<b>Bond Lengths (Å)</b>		
Cu-21N	2.297	2.237
Cu-22N	2.442	2.588
Cu-43N	2.298	2.239
Cu-44N	2.442	2.57
Cu-60N	2.223	2.198
Cu-61N	2.223	2.195
<b>Bond Angles (°)</b>		
21N-Cu-22N	70.3	68.8
21N-Cu-43N	162.9	156
21N-Cu-44N	96.5	92.4
21N-Cu-60N	98.1	100.8
21N-Cu-61N	95.5	98
22N-Cu-43N	96.5	91.9
22N-Cu-44N	82.4	78.7
22N-Cu-60N	168.1	169.6
22N-Cu-61N	102.1	103.6
43N-Cu-44N	70.3	69.1
43N-Cu-60N	95.4	98.2
43N-Cu-61N	98.1	100.5
44N-Cu-60N	102.1	102.8
44N-Cu-61N	168.1	169.5
60N-Cu-61N	75.7	76.9

According to the calculation results, there are six coordinate-covalent bonds around the copper atom in complexes. Interaction energies ( $E_{\text{Interaction}}$ ), formation enthalpies

$$E_{\text{Interaction}} = E_{\text{Complex}} - (E_{\text{Metal}} + E_{\text{Ligand}}) \quad (1)$$

$$H_{\text{Formation}} = H_{\text{Complex}} - (H_{\text{Metal}} + H_{\text{Ligand}}) \quad (2)$$

$$G_{\text{Formation}} = G_{\text{Complex}} - (G_{\text{Metal}} + G_{\text{Ligand}}) \quad (3)$$

( $H_{\text{Formation}}$ ) and formation Gibbs free energy ( $G_{\text{Formation}}$ ) of mentioned complexes are calculated by using Eqs. (1)-(3) and given in Table 2.

**Table 2.** Interaction energies ( $E_{\text{Interaction}}$ ), formation enthalpies ( $H_{\text{Formation}}$ ) and formation Gibbs free energy ( $G_{\text{Formation}}$ ) of mentioned complexes at B3LYP/6-31G(d,p)(LANL2DZ).

For Interaction energies				
	$E_{\text{Complex}}^a$	$E_{\text{Metal}}^a$	$E_{\text{Ligand}}^a$	$E_{\text{Interaction}}^b$
Complex (1)	-2859.974420	-195.079691	-2663.836033	-2.78x10 <sup>3</sup>
Complex (2)	-3370.175243	-195.079691	-3173.977726	-2.93x10 <sup>3</sup>
For formation enthalpies				
	$H_{\text{Complex}}^a$	$H_{\text{Metal}}^a$	$H_{\text{Ligand}}^a$	$H_{\text{Formation}}^b$
Complex (1)	-2859.973475	-195.078727	-2662.833199	-5.41x10 <sup>3</sup>
Complex (2)	-3370.174299	-195.078727	-3173.974892	-2.94x10 <sup>3</sup>
For formation Gibbs free energies				
	$G_{\text{Complex}}^a$	$G_{\text{Metal}}^a$	$G_{\text{Ligand}}^a$	$G_{\text{Formation}}^b$
Complex (1)	-2860.124723	-195.097596	-2664.013707	-2.66x10 <sup>3</sup>
Complex (2)	-3370.318803	-195.097596	-3174.150337	-2.81x10 <sup>3</sup>

<sup>a</sup> in atomic unit, <sup>b</sup> in kJ mol<sup>-1</sup>

According to the Table 2, interaction energies, formation enthalpies and formation Gibbs free energies are lower than zero. These results mean that formations of mentioned complexes are spontaneous and exothermic processes.

### 3.2. IR Spectra

In complex (1) and (2), there are 97 and 93 atoms, respectively. The number of active observable fundamentals of a non-linear molecule which contains N atoms is equal to (3N-6). Hence, 285 and 273 normal modes

of vibration are calculated for complex (1) and (2), respectively under C1 point group symmetry. Harmonic vibrational frequencies are calculated by using computational chemistry methods. Calculated frequencies are not scaled any factor. Some harmonic frequencies which have the higher intensity than 50 km mol<sup>-1</sup> are examined in detail and these results are given in Tables 3 and 4 for complex (1) and (2), respectively. IR spectra of complex (1) and (2) are represented in Fig. 2(a) and 2(b), respectively.

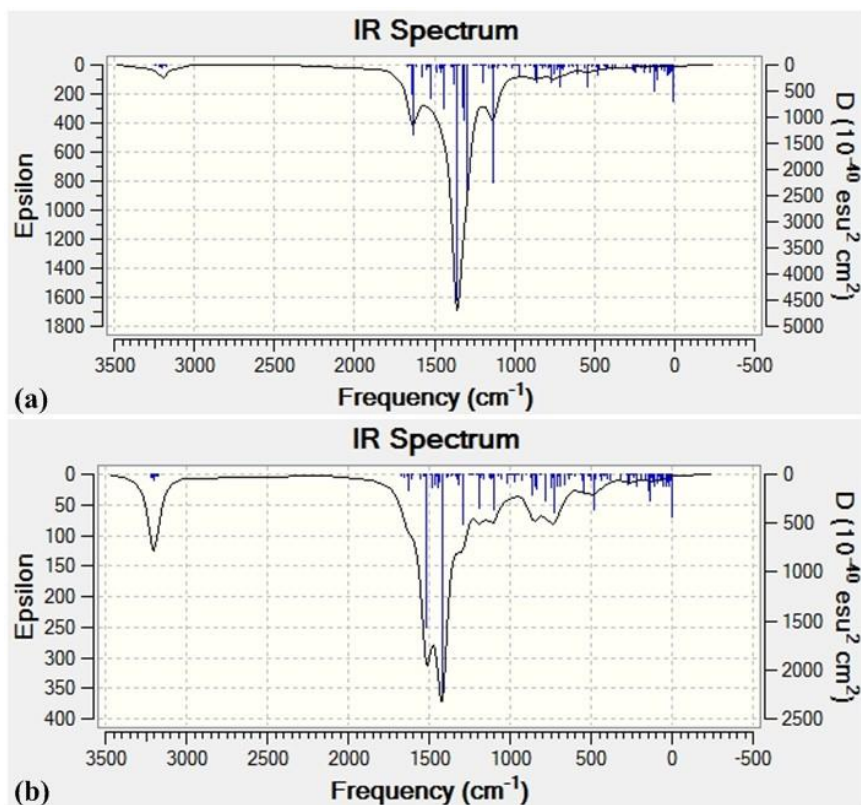


Figure 2. IR spectra of (a) complex (1) and (b) complex (2) at same level of theory in vacuo.

Table 3. Harmonic vibrational frequencies of complex (1) at B3LYP method in gas phase.

Mode	Frequency	Intensity <sup>a</sup>	Assignments
76	546	56.8621	$\omega_{C-H}$
98	720	72.8322	$\omega_{C-H}$
106	765	66.5457	$\omega_{C-H}$
122	862	69.6999	$\omega_{C-H}$ , $\nu_{C-N}$
126	866	58.9163	$\omega_{C-H}$ , $\nu_{C-N}$
136	971	57.2214	$\nu_{C=C}$ , $\omega_{C-H}$
170	1129	147.415	$\gamma_{C-H}$
172	1133	640.4009	$\nu_{C-N}$ , $\gamma_{C-H}$
173	1196	99.8947	$\gamma_{C-H}$ , $\nu_{C-N}$
194	1296	870.2322	$\nu_{C-N}$ , $\gamma_{C-H}$
196	1316	350.5012	$\gamma_{C-H}$
198	1328	270.3557	$\nu_{C=C}$ , $\omega_{C-H}$
202	1357	1436.2881	$\nu_{C=C}$ , $\nu_{N=O}$ , $\gamma_{C-H}$
203	1359	1055.3766	$\gamma_{C-H}$ , $\nu_{N=O}$ , $\nu_{C-N}$
205	1361	1537.638	$\nu_{C=C}$ , $\nu_{N=O}$
208	1376	121.3688	$\nu_{N=O}$
214	1442	297.1527	$\nu_{C-N}$
218	1461	50.6319	$\gamma_{C-H}$
222	1486	52.8916	$\gamma_{C-H}$
226	1521	245.2443	$\gamma_{C-H}$ , $\nu_{C=C}$
234	1576	87.5921	$\nu_{N=O}$ , $\nu_{C=C}$
238	1627	91.3218	$\nu_{C=C}$ , $\gamma_{C-H}$
240	1634	549.3618	$\nu_{C=C}$ , $\nu_{N=O}$
242	1638	231.2338	$\nu_{C=C}$ , $\nu_{N=O}$
245	1642	64.519	$\nu_{C=C}$ , $\nu_{N=O}$

Vibration modes:  $\nu$ , stretching;  $\gamma$ , rocking;  $\omega$ , wagging. <sup>a</sup> in  $\text{km mol}^{-1}$

**Table 4.** Harmonic vibrational frequencies of complex (2) at B3LYP method in gas phase.

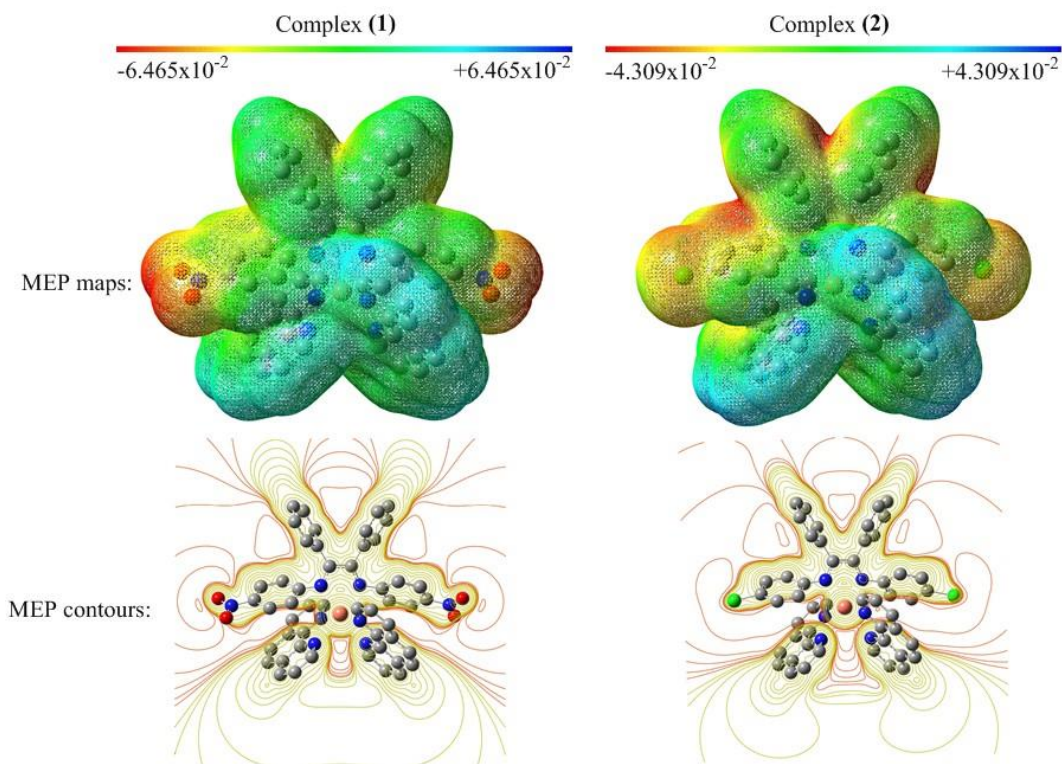
Mode	Frequency	Intensity <sup>a</sup>	Assignments
95	725	71.0678	$\omega_{C-H}$
105	785	53.6326	$\omega_{C-H}$
158	1103	99.9776	$\nu_{C-Cl}, \nu_{C=C}, \gamma_{C-H}$
172	1186	104.6714	$\gamma_{C-H}, \nu_{C-N}$
184	1289	166.6803	$\nu_{C-C}, \nu_{C-N},$
202	1419	806.6099	$\nu_{C-N}, \gamma_{C-H}, \nu_{C=C}$
212	1484	51.1067	$\gamma_{C-H}, \nu_{C=C}$
216	1517	593.3464	$\gamma_{C-H}, \nu_{C=C}$
230	1631	69.2755	$\nu_{C=C}$
256	3196	51.1024	$\nu_{C-H}$

Vibration modes:  $\nu$ , stretching;  $\gamma$ , rocking;  $\omega$ , wagging. <sup>a</sup> in  $\text{km mol}^{-1}$

### 3.3. Molecular Electrostatic Potential (MEP) Maps, MEP Contours and Single Occupied Molecular Orbital

Different values of the electrostatic potential at MEP map are represented by different colors which are red, yellow, green, light blue and blue. The red and yellow regions in MEP map are related to higher electron

density, while light blue and blue regions in MEP map is related to lower electron density. In MEP contours, there are two color lines which are yellow and red and these line related to positive charges and negative charges, respectively. Additionally, the steric effect can be easily seen from MEP contour. MEP maps and contours are represented in Fig. 3.

**Figure 3.** MEP maps and contours of mentioned complexes at B3LYP method in gas phase.

Electrons are more intense on  $-\text{NO}_2$  group than rest atoms or groups in complex (1). As for the complex (2), electrons are more intense on benzene rings which belong to  $\text{L}^2$  ligand than rest of the complex. A part of molecular orbital (MO) energy diagram of complex (1) and (2) are given in Figs. 4 and 5, respectively. Degeneracy tolerance is taken as  $2.6255 \text{ kJ mol}^{-1}$  in these diagrams. This value means that if energy difference between molecular orbitals is equal or lower

than  $2.6255 \text{ kJ mol}^{-1}$ , these molecular orbitals are taken as identical orbitals. According to this figure, 221 alpha-MO in complex (1) and 215 alpha-MO in complex (2) are single occupied molecular orbitals (SOMOs). Additionally, 219 and 220 alpha-MO are equivalent in complex (1) while 213 and 214 alpha-MO are equivalent in complex (2). Contour diagrams of SOMOs which belong to complex (1) and (2) are represented in Fig. 6.

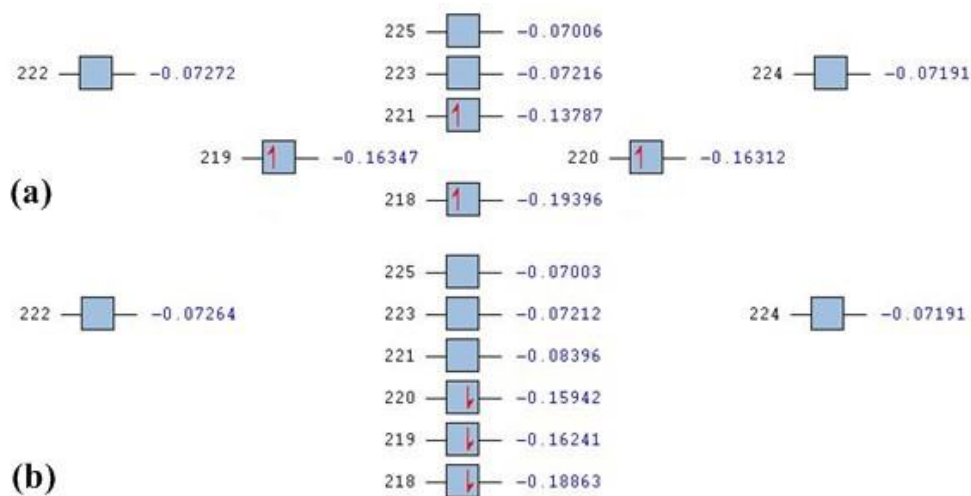


**Figure 4.** Energy diagrams of (a) alpha molecular orbitals and (b) beta molecular orbitals of complex (1) at same level of theory.

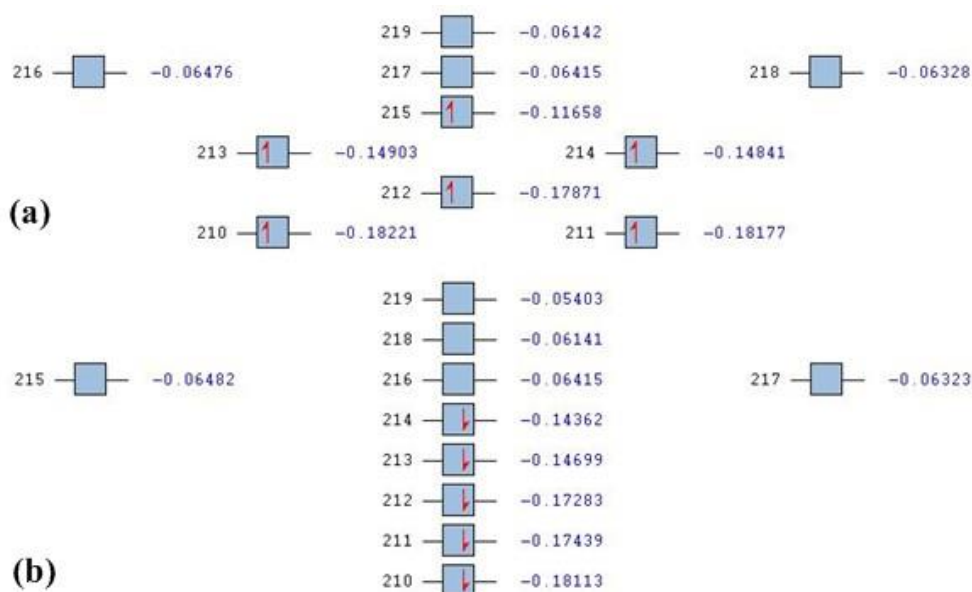


**Figure 5.** (a) alpha molecular orbitals and (b) beta molecular orbitals energy diagrams of complex (2) at same level of theory.

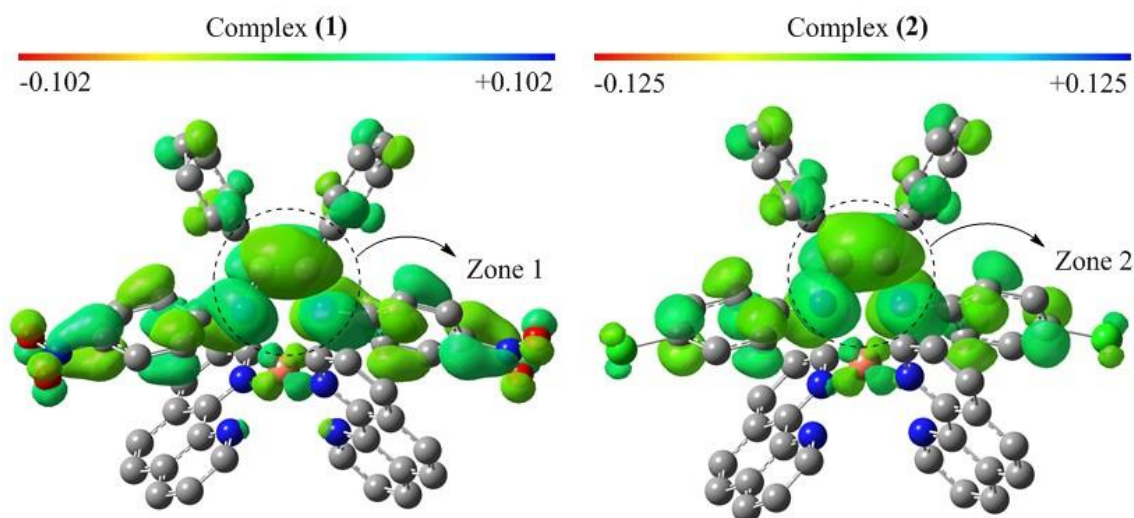


**Figure 6.** Contour diagrams of SOMOs for complex (1) and (2) at B3LYP method in gas phase.

According to Fig. 6, the electron of SOMO is mainly delocalized on  $L^1$  and  $L^2$  ligands in complex (1) and (2), respectively. Different values of electron density on contour diagrams are presented by different colors. Additionally, there are different lobes which have the different size in contour diagrams. Size variation means that electrons are more localized in big lobe than small lobe. As a result, SOMO electron is mainly localized on

zone 1 and zone 2 in  $L^1$  and  $L^2$  ligands, respectively.

### 3.4. UV-VIS Spectra

UV-VIS spectra of mentioned complexes are calculated by using time – dependent (TD) B3LYP method with 6-31G(d,p)(LANL2DZ) basis set in the gas phase. Calculated UV-VIS spectra of mentioned complexes are represented in Fig. 7.

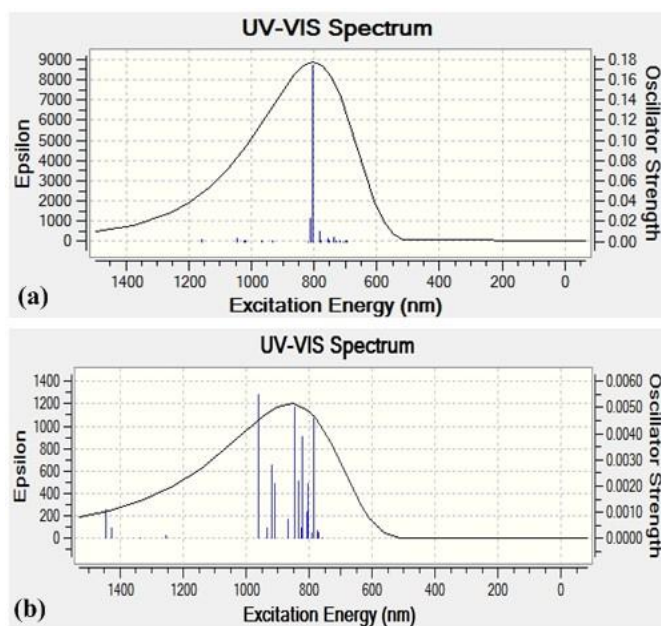


**Figure 7.** Calculated UV-VIS spectra of (a) complex (1) and (b) complex (2) at TD-B3LYP method in gas phase.

According to mentioned figure, main band for complex (1) is mainly occurred from a peak which wavelength is 803.4 nm, while main band for complex (2) is mainly occurred from three peaks. Their wavelengths are 962.3, 846.9 and 785.1 nm which have higher intensity than 1000 Epsilon. Each peak occurs from many electronic transitions. These transitions and their percentage of transition character (TC%) are

given in Table 5. TC% are calculated by using Eq. (4) [24-27].

$$TC\% = \frac{t^2}{\sum t^2} \times 100 \quad (4)$$

where t is coefficient of the wavefunction for each excitation and  $\sum t^2$  is the sum of the squares of all coefficient of the wavefunction for each excitation in a specific band.

**Table 5.** Ground state and excited state for main peak in complex (2) – (6), contribution values of relevant transitions and transition types of main peak.

Complexes	Wavelength (nm)	Ground State	Excited State	Contribution%	Transition Type	
Complex (1)	803.4	221 $\alpha$	226 $\alpha$	80.14	L $\rightarrow$ L <sup>a</sup>	
		220 $\beta$	223 $\beta$	18.55	L $\rightarrow$ L <sup>a</sup>	
		220 $\beta$	226 $\beta$	1.31	L $\rightarrow$ L <sup>a</sup>	
	Complex (2)	785.1	213 $\alpha$	216 $\alpha$	16.57	MLCT <sup>b</sup>
			213 $\alpha$	218 $\alpha$	6.62	MLCT <sup>b</sup>
			213 $\alpha$	219 $\alpha$	1.99	MLCT <sup>b</sup>
			214 $\alpha$	216 $\alpha$	28.41	L $\rightarrow$ L <sup>a</sup>
			214 $\alpha$	218 $\alpha$	1.33	L $\rightarrow$ L <sup>a</sup>
			213 $\beta$	215 $\beta$	1.30	L $\rightarrow$ L <sup>a</sup>
			213 $\beta$	216 $\beta$	3.30	L $\rightarrow$ L <sup>a</sup>
213 $\beta$			217 $\beta$	6.81	L $\rightarrow$ L <sup>a</sup>	
214 $\beta$			218 $\beta$	33.76	L $\rightarrow$ L <sup>a</sup>	
Complex (2)			846.9	213 $\alpha$	216 $\alpha$	27.18
	213 $\alpha$	219 $\alpha$		7.27	MLCT <sup>b</sup>	
	214 $\alpha$	216 $\alpha$		26.81	L $\rightarrow$ L <sup>a</sup>	
	214 $\alpha$	218 $\alpha$		12.83	L $\rightarrow$ L <sup>a</sup>	
	214 $\alpha$	219 $\alpha$		7.55	L $\rightarrow$ L <sup>a</sup>	
	213 $\beta$	215 $\beta$		2.60	L $\rightarrow$ L <sup>a</sup>	
	213 $\beta$	217 $\beta$		1.81	L $\rightarrow$ L <sup>a</sup>	
	213 $\beta$	219 $\beta$		12.88	L $\rightarrow$ L <sup>a</sup>	
	214 $\beta$	216 $\beta$		1.07	L $\rightarrow$ L <sup>a</sup>	
	Complex (2)	962.3		214 $\beta$	215 $\beta$	29.09
214 $\beta$			218 $\beta$	6.73	L $\rightarrow$ L <sup>a</sup>	
214 $\beta$			219 $\beta$	64.18	L $\rightarrow$ L <sup>a</sup>	

<sup>a</sup> Ligand to ligand charge transfer

<sup>b</sup> Metal to ligand charge transfer

Contour diagrams of molecular orbitals given in Table 5 are used for determination of transition type and these diagrams are given in supplementary material. According Table 5, main bands in UV-VIS spectra of complex (1) and (2) are mainly occurred from ligand to ligand charge transfer (LLCT).

### 3.5. <sup>1</sup>H- and <sup>13</sup>C-NMR Spectra

Chemical shifts in NMR spectra are recognized as an important part of the information contained and these data are valuable for structural interpretation due to their sensitivity to structural changes. Experimental NMR results of mentioned complexes are not given in literature. NMR spectra of mentioned copper(II) complexes are calculated at GIAO-B3LYP/6-

31G(d,p)(LANL2DZ) level in vacuum. Tetramethylsilane (TMS) is used as reference substance. TMS therefore is optimized at B3LYP/6-31G(d,p) level and chemical shifts of TMS are obtained at GIAO-B3LYP/6-31G(d,p) level. In all TMS calculations, T<sub>d</sub> point group is defined. Chemical shift ( $\delta$ ) values are calculated by using Eq. (5) [28],

$$\delta = \delta_{TMS} - \delta_{OUT} \quad (5)$$

where  $\delta$  is chemical shift value in ppm,  $\delta_{TMS}$  is the TMS reference and  $\delta_{OUT}$  is the value read from the Gaussian output file. Calculated chemical shift values of carbon atoms and hydrogen atoms are given in Table 6 and 7 for complex (1) and (2).

**Table 6.** The calculated chemical shifts values of carbon atoms in <sup>13</sup>C-NMR spectra for mentioned complexes.

Atoms <sup>a</sup>	Complex (1)	Complex (2)	Atoms <sup>a</sup>	Complex (1)	Complex (2)
1C	88.4757	88.6398	46C	90.9102	90.3029
2C	99.4719	98.7205	47C	95.5203	96.0637
3C	93.2863	93.1955	48C	104.4518	105.4741
4C	108.4021	108.0543	49C	97.3111	97.7514
5C	112.4217	113.5407	50C	90.6922	90.1842
6C	91.3248	91.1835	51C	90.9102	90.3096
7C	108.0799	109.0596	52C	89.3399	87.9338
8C	93.2075	92.8962	53C	90.6908	90.2130
9C	91.9178	91.4001	54C	97.3118	97.7748
10C	99.5809	98.5526	55C	104.4537	105.4639
12C	87.7875	86.7788	56C	95.5216	96.0133
13C	111.2268	111.3090	57C	117.9581	116.1169
23C	88.4737	88.6491	58C	117.9675	115.7514
24C	99.4713	98.6865	61C	122.9481	117.2802
25C	93.2860	93.1512	62C	122.9556	117.1410
26C	108.4025	108.0462	63C	89.5888	90.5864
27C	112.4288	113.4175	64C	87.8713	90.7445
28C	91.3247	91.1405	65C	102.8512	94.9589
29C	108.0835	108.9378	66C	87.2228	90.0813
30C	93.2072	92.9000	67C	85.9891	87.5906
31C	91.9172	91.4454	68C	89.5826	90.7387
32C	99.5809	98.5560	69C	87.8722	90.7348
34C	87.7848	86.8208	70C	102.8499	94.9515
35C	111.2293	91.3128	71C	87.2240	90.0726
45C	89.3400	87.9481	72C	85.9881	87.5808

<sup>a</sup> These atoms are represented in Fig. 1.

**Table 7.** The calculated chemical shifts values of carbon atoms in <sup>1</sup>H-NMR spectra for mentioned complexes.

Atoms <sup>a</sup>	Complex (1)	Complex (2)	Atoms <sup>a</sup>	Complex (1)	Complex (2)
(1C)H	7.0496	7.0429	(46C)H	6.0207	5.9712
(2C)H	7.1836	7.1154	(47C)H	6.3605	6.3837
(5C)H	9.2785	9.5988	(49C)H	5.8541	5.8621
(6C)H	6.7208	6.7042	(50C)H	5.8545	5.7853
(9C)H	6.6259	6.6008	(51C)H	6.0207	5.9772
(10C)H	6.8833	6.7898	(52C)H	5.9019	5.8117
(12C)H	6.3819	6.1937	(53C)H	5.8543	5.7930
(13C)H	7.6286	7.4620	(54C)H	5.8539	5.8715
(23C)H	7.0495	7.0510	(56C)H	6.3607	6.3976
(24C)H	7.1834	7.1240	(63C)H	6.1637	6.2909
(27C)H	9.2797	9.5805	(64C)H	6.1860	5.1026
(28C)H	6.7206	6.7103	(66C)H	5.7205	4.6416
(31C)H	6.6258	6.6044	(67C)H	4.2106	4.3909
(32C)H	6.8831	6.7854	(68C)H	6.1628	6.3024
(34C)H	6.3814	6.1916	(69C)H	6.1863	5.0680
(35C)H	7.6274	7.4671	(71C)H	5.7203	4.6783
(45C)H	5.9021	5.8033	(72C)H	4.2109	4.4544

<sup>a</sup> These atoms are represented in Fig. 1.

Aromatic hydrogen and carbon atoms give peaks in range 8 – 6 ppm and 145 – 110 ppm, respectively [29]. Additionally, aromatic hydrogen and carbon atoms can give peaks in range 7 – 4 ppm and 111 – 74 ppm, respectively in transition metal complexes in which center atom is very important in determination of chemical shift values of hydrogen and carbon atoms [29]. According to Tables 6 and 7, calculated chemical shift values are appropriate with theoretical expectations. Chemical shift values of hydrogen and carbon atoms imply that electronic structures of mentioned complexes are very close to each other. Chemical shift differences between mentioned complexes comprise around 65C and 70C atoms due to the substituent effect.

#### 4. CONCLUSIONS

The first calculations are performed with UFF method and the optimized structures of Cu(II) complexes are calculated by using B3LYP method with GEN keyword in vacuum. The structural parameters are obtained from the optimized structures. The IR spectrum for each complex is examined in detail. The electronic absorption spectra for mentioned complexes are calculated by using TD-B3LYP method

with LANL2DZ for metal atoms and 6-31G(d,p) for rest atoms in complexes. NMR spectra are calculated by using GIAO method and tetramethylsilane are used as reference substance. The interaction energies, formation enthalpies and formation Gibbs free energies are calculated and their values are lower than zero. These results show that formations of mentioned complexes are spontaneous and exothermic processes.

#### Acknowledgments

The numerical calculations reported in this paper are performed at TUBITAK ULAKBIM, High Performance and Grid Computing Center (TRUBA Resources).

#### REFERENCES

- [1] Zhang Y.Y., Ren N., Xu S.L., Zhang J.J., Zhang D.H., A series of binuclear lanthanide (III) complexes: crystallography, antimicrobial activity and thermochemistry properties studies *Journal of Molecular Structure* 2015; 1081: 413-25.
- [2] Protogeraki C., Andreadou E.G., Perdih F., Turel I., Pantazaki A.A., Psomas G.,

- Cobalt(II) complexes with the antimicrobial drug enrofloxacin: Structure, antimicrobial activity, DNA- and albumin-binding European Journal of Medicinal Chemistry 2014; 86: 189-201.
- [3] Zamani F., Zendehtdel M., Mobinikhaledi A., Azarkish M., Complexes of N,N-bis (salicylidene) 4,5-dimethyl-1,2-phenylenediamine immobilized on porous nanomaterials: Synthesis, characterization and study of their antimicrobial activity Microporous and Mesoporous Materials 2015; 212: 18-27.
- [4] Babahan I., Emirdağ-Öztürk S, Poyrazoğlu-Çoban E, Spectroscopic and biological studies of new mononuclear metal complexes of a bidentate NN and NO hydrazone-oxime ligand derived from egonol Spectrochimica Acta Part A: Molecular and Biomolecular Spectroscopy 2015; 141: 300-6.
- [5] Vural H., Uçar I., A combined theoretical and experimental study of chelidamate cadmium (II) complex,  $[Cd_2(dpa)_2(chel)_2] \cdot 2[Cd(dpa)(chel)] \cdot 6H_2O$  Spectrochimica Acta Part A: Molecular and Biomolecular Spectroscopy 2015, 136, 1298-307.
- [6] Demirbaş U, Bayrak R, Piskin M, Akçay H.T., Durmus M, Kantekini H., Synthesis, photophysical and photochemical properties of novel tetra substituted metal free and metallophthalocyanines bearing triazine units Journal of Organometallic Chemistry 2013; 724: 225-34.
- [7] Kumar V, Ahamad T, Nishat N, Some *O,O',O'',O'''*-di/tetra aryldithioimidophonate transition metal complexes derived from catechol and bisphenol-A as antibacterial and antifungal agents European Journal of Medicinal Chemistry 2009; 44: 785-93.
- [8] Raman N., Mahalakshmi R., Bio active mixed ligand complexes of Cu(II), Ni(II) and Zn(II): Synthesis, spectral, XRD, DNA binding and cleavage properties Inorganic Chemistry Communications 2014; 40: 157-63.
- [9] Sayin K., Karakas D., Karakus N., Alagöz Sayin T., Zaim Z., Erkan Kariper S., Spectroscopic investigation, FMOs and NLO analyses of Zn(II) and Ni(II) phenanthroline complexes: A DFT approach Polyhedron 2015; 90: 139-46.
- [10] Üngördü A., Tezer N., Effect on frontier molecular orbitals of substituents in 5-position of uracil base pairs in vacuum and water, Journal of Theoretical and Computational Chemistry 2017; 16: 1750066.
- [11] Ozbakir Isin D., Karakuş N., Quantum chemical study on the inhibition efficiencies of some sym-triazines as inhibitors for mild steel in acidic medium, Journal of the Taiwan Institute of Chemical Engineers 2015; 50: 306-13.
- [12] Sun J., ding J., Liu N., Yang G., Li J., Detection of multiple chemicals based on external cavity quantum cascade laser spectroscopy, Spectrochimica Acta Part A: Molecular and Biomolecular Spectroscopy 2018; 191: 532-38.
- [13] Üngördü A., Tezer N., DFT study on metal-mediated uracil base pair complexes, Journal of Saudi Chemical Society 2017; 21: 837-44.
- [14] Zhu Q., Wen K., Feng S., Guo X., Zhang J., Benzimidazobenzothiazole-based highly-efficient thermally activated delayed fluorescence emitters for organic light-emitting diodes: A quantum-chemical TD-DFT study, Spectrochimica Acta Part A: Molecular and Biomolecular Spectroscopy, 2018; 192: 297-303.

- [15] GaussView 5.0, Gaussian Inc., Wallingford, CT, USA, 2009.
- [16] Gaussian 09, rev. C.01, Gaussian Inc., Wallingford, CT, USA, 2010.
- [17] PerkinElmer, 2012. ChemBioDraw Ultra Version (13.0.0.3015), CambridgeSoft Waltham, MA, USA.
- [18] Rappe A.K., Casewit C.J., Colwell K.S., Goddard III W.A., Skiff W.M., UFF, a full periodic table force field for molecular mechanics and molecular dynamics simulations Journal of the American Chemical Society 1992; 114: 10024-35.
- [19] Becke A.D., Density-functional thermochemistry. III. The role of exact Exchange The Journal of Chemical Physics 1993, 98, 5648-5652.
- [20] Lee C., Yang W., Parr R.G., Development of the Colle-Salvetti correlation-energy formula into a functional of the electron density Physical Review B 1988; 37: 785-9.
- [21] Jr. Dunning T.H., Hay. P. J., Schaefer III H.F., (Eds). in Modern Theoretical Chemistry, Vol. 3, Plenum, New York, 1977.
- [22] Hay P. J., Wadt W.R., *Ab initio* effective core potentials for molecular calculations. Potentials for the transition metal atoms Sc to Hg The Journal of Chemical Physics 1985; 82: 270-83.
- [23] Wadt W.R., Hay P. J., *Ab initio* effective core potentials for molecular calculations. Potentials for main group elements Na to Bi The Journal of Chemical Physics 1985; 82: 284-298.
- [24] Sayin K., Karakaş D., Method/Basis Set Investigation and Spectral Studies for Oximate-Bridged trans-Platinum(II) Dimer Used as Anticancer Drug Journal of New Results in Science 2015; 8: 1-12.
- [25] Sayin K., Erkan Kariper S., Alagöz Sayin T., Karakas D., Theoretical spectroscopic study of seven zinc(II) complex with macrocyclic Schiff-base ligand Spectrochimica Acta Part A: Molecular and Biomolecular Spectroscopy 2014; 133: 348-56.
- [26] Sayin K., Karakaş D., Determination of structural and electronic properties of [Ni(NQSC)<sub>2</sub>] and [Ni(NQTS)<sub>2</sub>] complexes with DFT method Journal of New Results in Science 2013; 2: 47-53.
- [27] Sayin K., Karakaş D., Quantum Chemical Studies on [Co(ntb)(pic)]<sup>+</sup> Complex Ion Journal of New Results in Science 2013; 2: 54-9.
- [28] Güveli Ş., Özdemir N., Bal-Demirci T., Ülküseven B., Dinçer M., Quantum-chemical, spectroscopic and X-ray diffraction studies on nickel complex of 2-hydroxyaceto phenone thiosemi carbazone with triphenylphosphine Polyhedron 2010; 29: 2393-403.
- [29] Erdik E., Organik Kimyada Spektroskopik Yöntemler, 2nd Edition, Gazi Kitabevi: Ankara, Turkey, 1998.